



Combustion characteristics of high ash Indian thermal, heat affected coal and their blends

Subhajit Aich¹ · Barun Kumar Nandi¹ · Sumantra Bhattacharya¹

Received: 13 June 2020/Revised: 16 October 2020/Accepted: 8 March 2021/Published online: 9 April 2021
© The Author(s) 2021

Abstract Onsite mine fire generates large volumes of heat-affected coal in Jharia coalfields, India. Direct utilization of such heat-affected coal in thermal utilities is not feasible as such coal does not have the desirable volatile matter required for combustion. In the present work, experimental studies have been carried out to investigate the possible utilization of such heat-affected coal in thermal utilities by blending with other coal. Heat-affected coal (31% ash and 5300 kcal/kg GCV) collected from Jharia coalfield were blended with thermal coal (28% ash and 5650 kcal/kg GCV) in different ratios of 90:10, 80:20, 70:30 and 60:40 to identify the desirable blend ratio for burning of blended coal in thermal utilities. Burning characteristics of all the coals were carried out using TGA. Various combustion parameters such as ignition temperature, peak temperature, burnout temperature, ignition index, burnout index, combustion performance index, rate and heat intensity index of the combustion process and activation energy were evaluated to analyse the combustion process. Experimental and theoretical analysis shows the blend ratio of 90:10 can be used in place of only thermal coal in utilities to reduce the fuel cost.

Keywords Coal blends · Heat affected coal · Combustion indices · TGA-DTG · Burning profile · Mass gain analysis

1 Introduction

Large volumes of thermal coal and metallurgical coal reserves with gross calorific value (GCV) above 5500 kcal/kg are located in the eastern Indian states of West Bengal and Jharkhand. Coal mines in these two states are besieged with the problem of a non-utilized coal, known as “Jhama” coal (local nomenclature). Jhama coal or heat affected coking coal is a thermally altered metamorphosed coal found mainly in Damodar Valley coalfields of Jharia and to a certain extent in Raniganj, which are a part of the Lower Gondwana coalfields in the eastern Indian states of Jharkhand and West Bengal. This alteration of coking coal is due

to the effect of high temperature igneous intrusion, magmatic heating and direct contact with igneous rock (Singh et al. 2007). This intrusion causes dramatic changes in vitrinite reflectance, mineralogy and geochemistry of the coal seams which affects the physical, chemical and microscopic properties (Onifade et al. 2019). Following intrusion, a major change in the evacuation of volatile matter (VM) is observed that results in deposition of carbonaceous matter which is the reason heat affected coal has been generally observed to show an increase in ash and fixed carbon (Nag et al. 2011). Macroscopical observation revealed that Jhama coal is dull, hard and compact with its pores either empty or filled with mineral matter (Nag et al. 2009). A Jhama coal, also known as natural burnt coke has little VM which makes it non-combustible friendly (Singh et al. 2016). Jhama being partially pseudo carbonized is expected to lose all its caking and swelling properties. Having quite difficult washability characteristics due to uniform distribution of mineral matters in the partially carbonized coal matrix, its large scale application in coke

✉ Barun Kumar Nandi
bknandi2004@gmail.com; barun@iitism.ac.in

¹ Department of Fuel Minerals and Metallurgical Engineering,
Indian Institute of Technology (Indian School of Mines),
Dhanbad 826004, Jharkhand, India

making is a challenging issue (Chakladar et al. 2020). It was reported that Jhama coal had to undergo certain coal preparation practise to improve its quality as blend (Nag et al. 2009, 2011). Total reserves of Jhama coal, in the Jharia coalfield alone currently stands at 5313 Mt. About 39% of coking coal has been devolatilized due to igneous intrusion and 61% due to mine fires (Singh et al. 2007). Occurrence of large reserves of Jhama coal create problems in the development and production work in the coal mines alongside causing mine fire in an around the mines making Jharia coalfield one of the most polluted area of the country impacting severely the health of the local population. According to the report released by environmental activist group in January 2017, PM 10 level in Jharia was 295 $\mu\text{g}/\text{m}^3$ in 2017, almost three times the permissible limit of 100 $\mu\text{g}/\text{m}^3$, while the coal town of Dhanbad with a population of 1.16 million (2011 census) registered PM 10 at 238 $\mu\text{g}/\text{m}^3$ and was declared the ninth most polluted town in India. The figures underlie the significance of finding an alternate use of Jhama coal, e.g. as a blend to thermal coal for combustion purposes in utilities. That is the genesis of the present investigation.

Research work on the combustion of different types of coal blends has been carried out by many researchers (Shih and Frey 1995; Lv et al. 2006; Baek et al. 2014; Raaj et al. 2016; Li et al. 2017; Wang et al. 2017). Shih and Frey studied different types of theoretical models that can be used in coal blending to optimize the desired coal properties. Raaj et al. studied the results of various characterization studies of coal blends for effective use in thermal power plants. Lv et al. studied various equilibrium strategies based on coal blending methods for combined carbon and PM10 emission reductions. Li et al., have worked on the effect of ashing temperature and coal blending on ash sintering and fusion behaviour during combustion of Zhundong lignite coal. Wang et al. studied the influence of coal blending on ash fusion property and viscosity. Baek et al. reported the effect of the coal blending method in a coal fired boiler on carbon in ash and NO_x emission. All such studies used thermogravimetric analysis (TGA) to identify the desirable blend ratio of different coals. Based on TGA data, burning profiles of coals were obtained and used to identify the desirable blend ratio for combustion of two or more coals. However, all the studies were carried out with the emphasis on the environmental impact of coal burning or economy of coal blending process. Very little work is available in the published literature on utilization of “Jhama” coal as such and on its combustion characteristics in particular. For efficient utilization of Jhama coal, they may be blended with similar properties of thermal coal.

Combustion of coal and heat release from it is a complex phenomenon, which depends on various physico-

chemical characteristics of coal (Deng et al. 2015). Different burning parameters of coal like initial ignition temperature, coal burning rate and energy release rate could vary for each coal. These burning characteristics are mostly influenced by the types of hydrocarbon present in coal. Due to variation in rates of combustion, different coal, even of similar GCV, might need different residence time in the boiler for complete combustion and heat release. Types of hydrocarbon present in coal vary widely across different coal seams. Therefore, each coal burns with different residence time and heat release rate. Burning these types of coal might result in incomplete combustion, unburned carbon loss (in both bottom and fly ash) combined with associated environmental problems along with fuel loss and lower boiler efficiency. Hence, it is necessary to study the combustion compatibility of coal blends before feeding them to boiler. The present work aims to examine the scope of blending of a thermal coal and “Jhama” coal with similar heat values for combustion purpose so that the latter one could be consumed in utilities.

2 Experimental

Two representative Run of Mine (ROM) coal samples named here after as Sample A and Sample B were obtained from two different coal mines of Jharia, in Jharkhand, India. Sample A was a thermal coal and Sample B was a heat affected Jhama coal. Both the coals were carefully selected to ensure relatively close values of ash and GCV. ROM samples, -200 mm in size, were crushed in stages by Jaw Crushers to -12.7 mm size. Crushed samples were reduced in mass by standard coning and quartering sampling method. Then samples were crushed to -1 mm size by Double Roll Crusher. Further, -1 mm samples were pulverized to -72 mesh size. Sub-samples were collected from the pulverised mass for various analysis by the coning and quartering method. For blending experiment, sub-samples were prepared by mixing sample A and sample B in different weight ratios (90:10, 80:20, 70:30 and 60:40) using a laboratory blender. Subsequently, representative samples from the blends were collected by coning and quartering method. Samples A and B were carried characterised by proximate analysis, ultimate analysis, free swelling index (FSI) and GCV. Combustion behaviour was analysed by thermal analysis in a TGA analyser (Model: STA 449 F3 Jupiter; Make: NETZSCH, Germany) in the presence of O_2 environment at heating rate of 10 $^\circ\text{C}/\text{min}$ (60 mL/minute-flow rate).

Based on the TGA-DTG data, various burning profile parameters such as ignition temperature (T_i , $^\circ\text{C}$), peak temperature (T_p , $^\circ\text{C}$), burnout temperature (T_f , $^\circ\text{C}$) and peak burning rate (DTG_{max} , weight % per minute) were

evaluated (Aich et al. 2019a; Behera et al. 2020). Theoretically, T_i is defined as the temperature where the rate of weight loss accelerates due to beginning of combustion process. Peak temperature T_p is the temperature where the rate of weight loss is maximum, corresponding burning rate being DTG_{max} . T_f corresponds to burnout temperature, where the weight becomes constant at the completion of combustion. Further based on the TGA/DTG data, ignition index (D_i , weight % per minute³) and burnout index (D_f , weight % per minute⁴) are calculated as shown in Eqs. (1) and (2) (Zhang et al. 2015; Aich et al. 2020; Behera et al. 2019)

$$D_i = \frac{DTG_{max}}{t_p t_i} \quad (1)$$

$$D_f = \frac{DTG_{max}}{\Delta t_{1/2} t_p t_i} \quad (2)$$

where, DTG_{max} (weight % per minute) is the maximum burning rate that relates to T_p , t_p (minute) is the peak time zone corresponding to DTG_{max} (weight % per minute), t_i (minute) is time of ignition, $\Delta t_{1/2}$ is the time corresponding to 50% of peak combustion rate. $DTG/DTG_{max} = 0.5$, t_f (min) is the time of burn-out. Higher ignition index (D_i) infers, lower the peak time (t_p), and lower the temperature coal starts registering weight loss. Hence, higher ignition index is necessary for coal to be burned easily (Aich et al. 2019a). Higher value of D_i signifies the easy ignitibility of coal due to the presence of highly volatile hydrocarbon whereas lower value infers difficulty in coal burning. Similarly, higher D_f indicates better energy release and combustion rate due to faster chemical reactions between coal and O_2 /air. Following thermal analysis, two comprehensive index-parameters namely combustion performance index (S_f), and rate and intensity index of combustion process (H_f , can also be calculated by Eq. (3) and Eq. (4) (Aich et al. 2019b; Behera et al. 2019).

$$S = \frac{DTG_{max} DTG_{mean}}{T_i 2T_f} \quad (3)$$

$$H_f = T_p \ln \left(\frac{\Delta t_{1/2}}{DTG_{max}} \right) \quad (4)$$

where, DTG_{mean} is the mean combustion rate. The performance index (S) is a measure of ignition combustion and burn-out properties of coal. Lower values of T_i & T_f results in higher value of S_f , which represents good combustion performance of fuel. H_f , denotes the energy rate of the combustion process. A lower number signifies good combustion performance.

Combustion of fuel is a chemical reaction between fuel and oxygen and as such, analysis of activation energy (E) of individual and blend samples are necessary to get an

insight of combustion and identify the optimal blending ratio. Various methods to analyse the activation energy for combustion have been proposed. However from literature it was observed that Coats-Redfern method is the most widely used model in analysing the activation energy (Behera et al. 2020; Ken et al. 2018; Aich et al. 2019a). The method utilized a first order Arrhenius law with a temperature function, according to $f(\alpha)$ - reaction model and $g(\alpha)$, the integral reaction model for determining the activation energy using the formula as shown in Eq. (5) as follows (Behera et al. 2020; Aich et al. 2019a).

$$\ln \frac{g(\alpha)}{T^2} = \ln \left(\frac{AR}{\beta E} \left[1 - \left(\frac{2RT}{E} \right) \right] \right) - \frac{E}{RT} \quad (5)$$

where, $g(\alpha)$ is the reaction model, α is the mass extent of reaction, m_0 , m_t , and m_∞ are initial sample mass, sample mass at time t , and sample mass at the end of reaction, respectively. T ($^\circ\text{C}$) is the temperature, R is the universal gas constant, E is the activation energy in kJ/mol, β is the linear heating rate and $\frac{2RT}{E} = 1$ is an approximation adopted in the Coats-Redfern (CR) method, A (S^{-1}) is the frequency factor. Extent of reaction (α) is determined from the TGA data as:

$$\alpha = \frac{m_0 - m_t}{m_0 - m_f} \quad (6)$$

By plotting $\ln \frac{g(\alpha)}{T^2}$ vs $1/T$ the slope equals to $-E/2.303R$ and from there the value of activation energy and pre-exponential factor can be evaluated by using the Eqs. (5) and (6).

3 Results and discussions

3.1 Characterization of coal samples

Table 1 shows that, both Sample A and sample B have relatively close values of ash and moisture. There is significant difference in volatile matter content, 19.43% for sample A and 7.66% for sample B. GCV and FSI values are also quite close. It is important to note that the presence of volatile matter in any fuel helps in burning. As a result, the calculated value of fuel ratio, 8.17, is also adverse for sample B. Both these negative attributes possibly explain the reluctance of utilities to accept the Jhama coal (sample B) for power generation. Ultimate analysis presented in Table 2 indicates that sample B contains 87.66% of carbon (C) compared to 84.22% in sample A. However, hydrogen content in sample A is higher (4.63%). Calculated values of H/C ratios are 0.66 and 0.32 for sample A and sample B, respectively. Lower values of H/C signifies dominance of C=C bond and C≡C bond in sample B compared to the C-

Table 1 Quality parameters analysis of sample A and B (40 °C, 60% Relative humidity)

Sample	Ash (%)	Moisture (%)	VM (%)	Fixed carbon (%)	Fuel ratio	GCV (kcal/kg)	FSI
A	31.47	0.83	19.43	48.27	2.49	5613	≤ 0.5
B	28.27	1.52	7.66	62.55	8.17	5343	≤ 0.5

Table 2 Elemental analysis of samples A and B on dry mineral matter free basis

Sample	Carbon (%)	Hydrogen (%)	Nitrogen (%)	Sulphur (%)	Oxygen (%)	H/C mole ratio
A	84.22	4.63	1.61	0.60	8.95	0.66
B	87.66	2.82	1.80	0.83	6.90	0.32

C bond and C-H bond. Also lower is the oxygen content of the heat affected Jhama coal, sample B.

3.2 TGA of individual samples

TGA plots are shown in Fig. 1 and Fig. 2 indicate practically no change in weight loss in the temperature region 30–150 °C, signifying very low level of moisture. These results are in line with the results obtained from proximate analysis (Table 1). After 150–350 °C range for sample A and after 400 °C for sample B, some weight gain is identified, possibly due to adsorption of oxygen gas in porous structure of the coal (Behera et al. 2020; Aich et al. 2019a). For sample A, O₂ adsorption is more compared to sample B, signifying the former thermal coal is more porous. Reduced porous structure in sample B further lowers the gas (CO₂/O₂) diffusion rate during combustion and reduces the rate of combustion. In sample A decrease in weight loss started from 350 °C due to the release of volatile matter (Aich et al. 2020). After 400 °C, sharp fall in weight loss

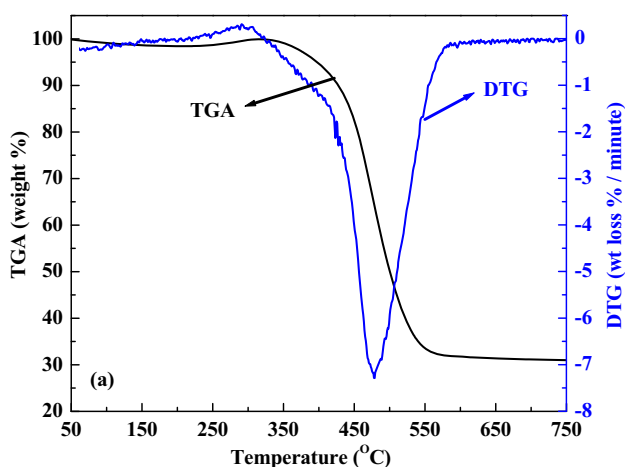


Fig. 1 Thermal curve of coal sample A at constant heating rate of 10 °C/minute

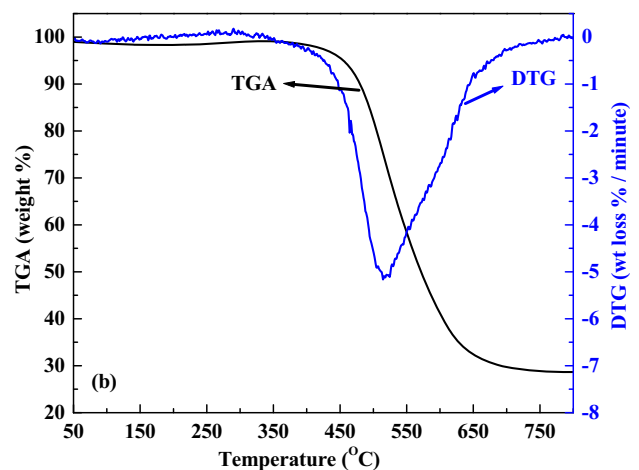


Fig. 2 Thermal curve of coal sample B at constant heating rate of 10 °C/ minute

signifies the beginning of combustion process. After 550 °C, weight loss becomes constant, suggesting end of combustion process with residue as ash. However, for sample B, decrease in weight loss started after 400 °C due to initiation of de-volatilization and sharp decrease in weight is observed after 450 °C as combustion process started. Combustion process was completed after attaining a temperature of 650 °C. To determine the characteristic temperatures during combustion, DTG analysis was performed and the results are also shown in Fig. 1 and 2. From DTG curves a clear variation in burning characteristics of two samples are observed. Burning temperature profiles, T_i , T_p and T_f for both the samples are listed in Table 3. From the table it can be observed that sample A started burning at lower temperature $T_i= 379$ °C (weight loss % per min) compared to 448 °C for sample B. Following variation in ignition temperature infers larger presence of VM (19.43%) in sample A compared to that in sample B (7.66%). During burning, higher amount of VM gets released from sample A, which starts burning easily and

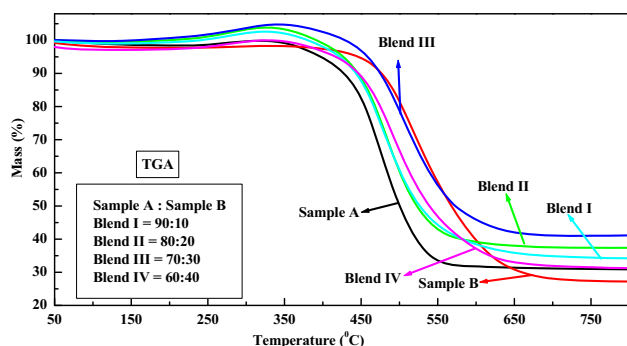
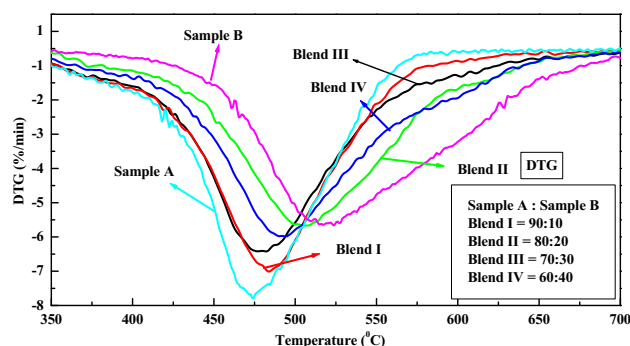
Table 3 Combustion temperatures and burning rate of sample A and B

Sample	T_i (°C)	T_p (°C)	T_f (°C)	DTG _{max} (wt% per minute)
Sample A	379	474	551	− 7.288
Sample B	448	514	644	− 5.162
Blend I; A:B = 90:10	384	484	564	− 6.508
Blend II; A:B = 80:20	392	484	585	− 5.866
Blend III; A:B = 70:30	411	494	614	− 5.484
Blend IV; A:B = 60:40	423	505	615	− 5.170

assist burning of sample at reduced temperature (Aich et al. 2019a). Obtained values of peak burning temperature T_p are 474 °C for sample A and 514 °C for sample B. Obtained values of DTG_{max} (weight % per min) for sample A is 7.28 and for sample B is 5.16. Lower value of sample B appears to be due to the relative absence of porous structure as well as volatiles in sample B compared to sample A (Alvarado et al. 2016). Single peaks in sample A and sample B in DTG curve signifies stage-wise smooth combustion with the removal of water, elimination of higher molecular weight hydrocarbons (Alvarado et al. 2016). T_f (burn-out temperature) for sample A and sample B are 551 °C and 644 °C, respectively. That shows sample B burns at a significantly lower rate with longer time for complete combustion. Higher burn-out temperature of coal signifies lower rate of heat release due to higher resistance to O_2 reaction that leads to waste un-burnt carbon.

3.3 TGA of coal blends

Experiments were carried out with blends of Sample A and sample B with different mass ratio of 90:10 (Blend I), 80:20 (Blend II), 70:30 (Blend III) and 60:40 (Blend IV) and corresponding TGA-DTG plots are shown in Fig. 3 and Fig. 4. Compared to samples A and B, no significant change in weight loss pattern in the temperature region 300–400 °C (Fig. 3) is observed. However, O_2 adsorption appears to be more in Blend I and II compared to Blend III

**Fig. 3** TG curves of coal sample A and B and their blends**Fig. 4** Differential-thermogravimetric curves of coal sample A and B and their blends

and IV due to the larger mass of Sample A in Blend I and Blend II. Various characteristic temperatures obtained for the Blends from Fig. 4 are summarized in Table 3. With the increase in Sample B mass percentage from 10% (Blend I) to 40% (Blend IV), T_i increases from 384 °C to 423 °C compared to the T_i for sample A (379 °C) and to sample B (448 °C). This increase in T_i appears to be due to the decrease in volatile matter in the Blends. Similar trends are observed for T_p with an increase from 484 °C (Blend I) to 505 °C (Blend IV), and for T_f due to the decrease in volatile matter of the Blends. Significant variation of T_i , T_p , T_f with blend ratios 1.0, 0.9, 0.8, 0.7 and 0.6 are shown in Fig. 5a, 5b and 5c. It can be observed that, T_i varies monotonously with blending ratio with the following generalized expression

$$T_i = 453.5 - 71 (\text{blend ratio}), R^2 = 0.9156 \quad (7)$$

Identical value of T_p , 484 °C is noted for blend ratios 0.8 and 0.9, though DTG_{max} are different, 5.86 wt% per min and 6.508 wt% per min, respectively (Table 3). It is inferred therefore that though T_p is same, burning rate could be different. Hence, maximum coal combustion rate apart from peak temperature is considered for determining optimum blend ratios of sample A and sample B. Overall however variation in T_p can be expressed as

$$T_p = 518.1 - 38.52 (\text{blend ratio}), R^2 = 0.8487 \quad (8)$$

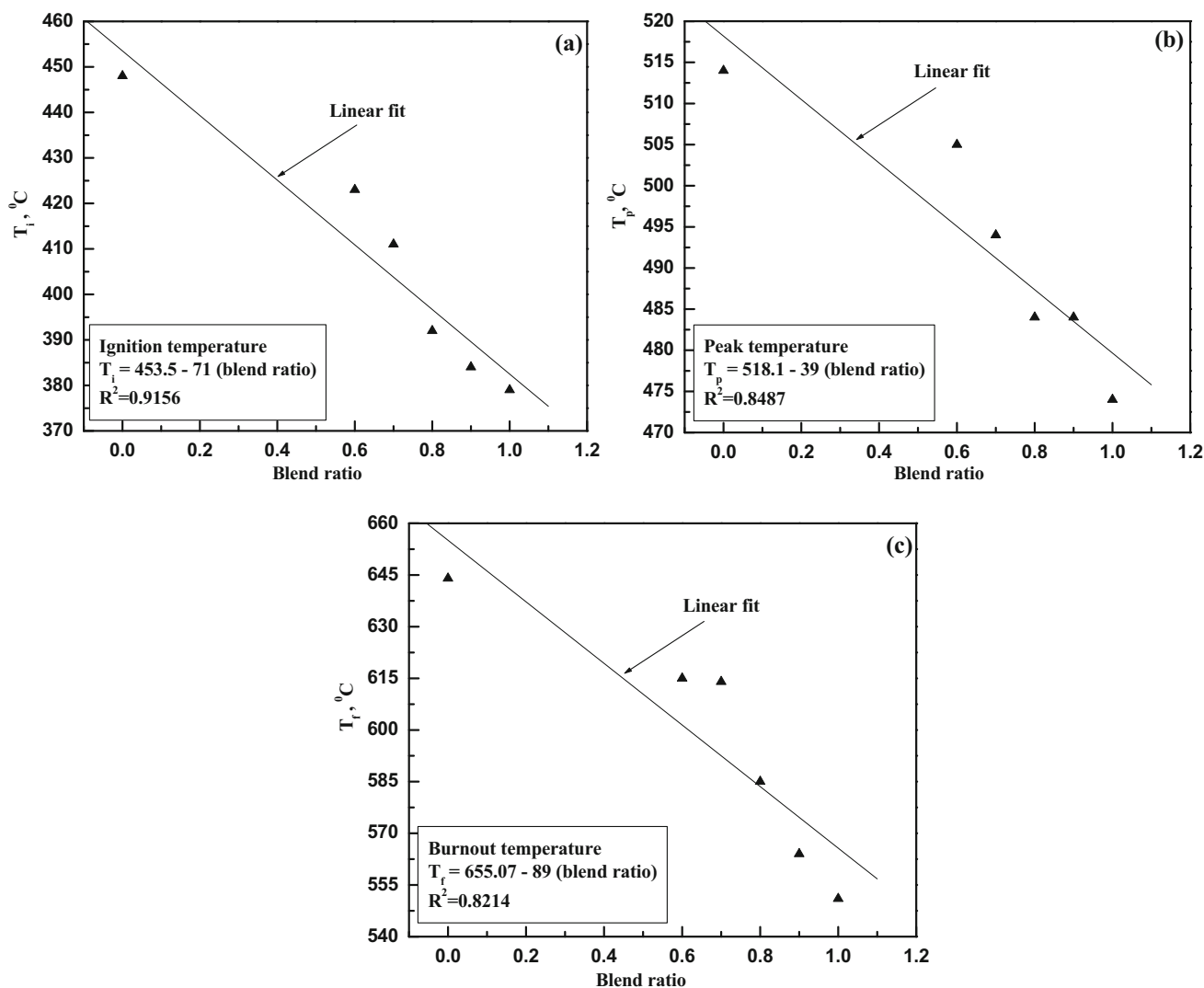


Fig. 5 Burning profiles (T_i , T_p , T_f) and blend ratio of sample A, B and their blends

Similar to T_p , analysis of T_f as shown in Fig. 5c indicates that, T_f increases linearly with decreasing blend ratio from 1.0 to 0.6. However, for Blends III and IV, variation of T_f is negligible (614 °C and 615 °C) with lower DTG_{max} for Blend IV. This appears to indicate that Blend IV, while showing lower peak combustion rate maintains a steady combustion rate and completes combustion along with Blend III. The same is also observed from Fig. 3. Overall, variation in T_f can be expressed as

$$T_f = 655.07 - 89 (\text{blend ratio}), R^2 = 0.8214 \quad (9)$$

Table 3 also shows the maximum combustion rate, (DTG_{max}) that varies from 6.50 wt% per min (Blend I) to 5.17 wt% per min (Blend IV) compared to 7.28 wt% per min and 5.16 wt% per min for samples A and B, respectively. This variation appears to be due to the variation in total combustible mass (VM and FC) as well as variation in

porous structure in the Blends. It can be further inferred from Table 3 that the values of T_p , and T_f for Blend I are quite close to those of Sample A. In common plant practice, maximum 15–20 °C variation of T_p and T_f are acceptable for different Blends. Hence, it can be concluded that Blend I can be used in place of sample A with insignificant variation in coal combustion rate.

3.4 Analysis of combustion characteristics parameters

The extent of combustion rate was further assessed by the analysis of different characteristics time and combustion parameters, t_i , t_p , t_f , $\Delta t_{1/2}$, D_i and D_f and are shown in Table 4. Burnout time t_f for sample A is 49.82 min compared to 59.64 min for sample B, possibly because the latter takes longer time for complete combustion. Higher

Table 4 Burning characteristic parameters of samples A and B and their blends

Sample	t_i (min)	t_p (min)	t_f (min)	$\Delta t_{1/2}$ (min)	D_i (10^{-3} wt% per min ³)	D_f (wt% per minute)
Sample A	32.64	42.09	49.82	38.96	– 5.30	– 0.89
Sample B	40.09	46.64	59.64	42.82	– 2.76	– 0.43
Blend I	32.89	42.86	50.87	38.97	– 4.61	– 0.76
Blend II	33.87	43.05	53.25	38.85	– 4.02	– 0.65
Blend III	36.20	44.48	56.58	40.24	– 3.40	– 0.54
Blend IV	36.58	45.04	56.13	40.49	– 3.13	– 0.50

residence time was attributed due to the presence of low volatile content and lower gas transport (CO_2/O_2) rate during combustion though pore diffusion in sample B. For blends with the increasing mass proportion of sample B from 10 to 40%, t_f increases from 50.87 min (blend I) to 56.13 min (Blend IV). Increase in t_f is due to the decrease in high volatile hydrocarbon content and lower gas diffusion rate (CO_2 and O_2) during combustion. It is observed that, $\Delta t_{1/2}$ values of blends occur in a span of 38.97–40.49 min which is in the range for Sample A (38.96 min) and sample B (42.82 min). The increase in $\Delta t_{1/2}$ signifies that, burning of blends are possibly not uniform in nature and the two components of the blend burn separately. Table 4 also shows the ignition index for sample A to be 5.30×10^{-3} and 2.76×10^{-3} wt% per min⁴ for sample B. Higher value of D_i infers that sample A combusted easily. For blends, with increase in mass percentage of sample B, D_i decreases from 4.61×10^{-3} (blend I) to 3.13×10^{-3} wt% per min⁴ (Blend IV). That appears to signify increasing difficulty in burning. For burnout index (D_f) it is observed that, except Blend II, other values are in between those for Sample A and sample B.

3.5 Analysis of combustion indices

To assess the combustion performance, H_f (rate and heat intensity index) and S_f (performance index) were evaluated using Eqs. (3) and (4), and the results are listed in Table 5. S_f for the blends appear in the mid-range (7.35×10^{-8} –

4.27×10^{-8} wt%² per min² °C³) of samples A (8.84×10^{-8} wt%² per min² °C³) and B (3.83×10^{-8} wt%² per min² °C³) suggesting that desired combustion performance can possibly be achieved. Likewise, trend is also observed for combustibles (FC + VM) versus non-combustibles (ash) ratio, (VM + FC)/Ash for both the samples and their blends. Sample A possesses very low H_f value of 1.95, which is a clear indication of good combustion performance. Sample B possess high H_f value of 2.33 °C suggests difficulty in combustion process. Only blend I have lower H_f of 2.05 °C compared to the other blends suggesting blend I theoretically provides better combustion performance among all the blends. It can be observed (Table 5) that comprehensive index of sample A have higher values of S_f (8.84×10^{-8} wt%² per min² °C³) and lower values of H_f (1.95 °C) compared to sample B. The results estimated are in accordance with the literature (Behera et al. 2020; Aich et al. 2019a, 2020), according to which a coal having the highest S_f value and lowest H_f value suggests better combustion behaviour since both the indices S_f and H_f are directly and inversely proportional to maximum combustion rate (DTG_{max}), respectively (Eqs. (3) and (4)). Among the blends maximum S_f and minimum H_f have been recorded for Blend I (90:10).

3.6 Analysis of activation energy

Analysis of activation energy for combustion of samples A and B and their blends were carried out using CR method

Table 5 Analysis of performance, intensity indices and combustible to non-combustible ratio

Sample	$S_f(10^{-8})$ wt% ² per min ² °C ³	H_f (°C)	(VM + FC)/Ash
Sample A	8.84	1.95	2.15
Sample B	3.83	2.33	3.59
Blend I	7.35	2.05	2.16
Blend II	6.26	2.09	2.70
Blend III	5.07	2.18	3.21
Blend IV	4.27	2.27	3.43

to get the optimum coal blending ratio (Fig. 6). Table 6 summarizes the results of kinetic parameters obtained from CR method. The table indicates that activation energies of blends lies within the activation energy range of sample A (106.48 kJ/mol) and sample B (129.34 kJ/mol). Lower activation energy of sample A is possibly due to high volatile content. High volatile matter helps in easy ignition of coal and reduces the activation energy for combustion

reaction. Sample B has higher content of fixed carbon that is difficult to ignite compared to volatiles and hence requires higher activation energy for combustion reactions. For blend samples it is observed that, activation energy increases from Blend I (114.89 kJ/mol) to Blend IV (124.99 kJ/mol) with increasing proportion of sample B in the blends. By and large activation energy for Blend I is

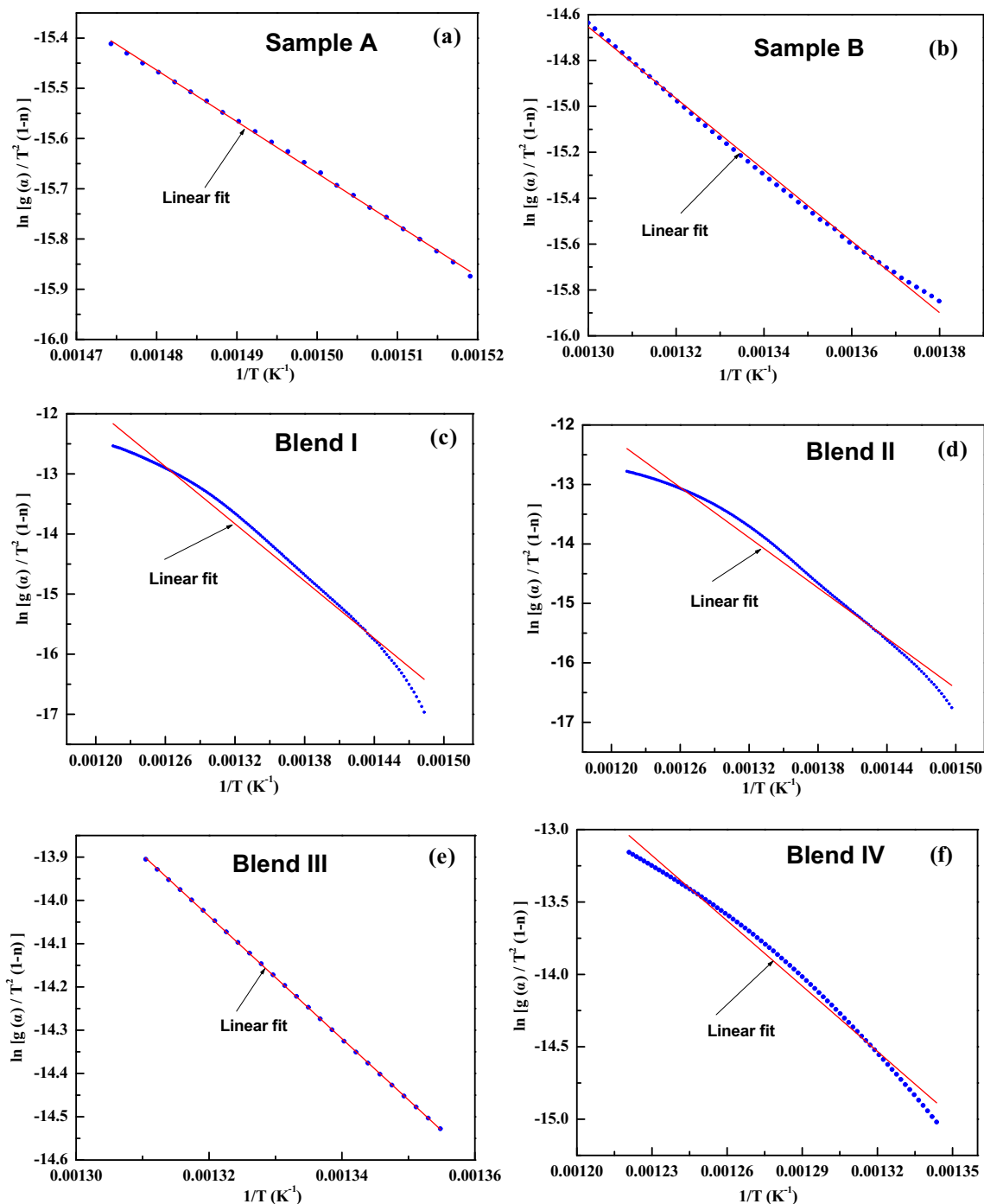


Fig. 6 Coats-Redfern plot of sample A, B and their blends

Table 6 Arrhenius equation parameters of sample A, B and their blends

Sample	<i>E</i> (kJ/mol)	<i>R</i> ²
Sample A	106.48	0.9985
Sample B	129.34	0.9956
Blend I	114.89	0.9694
Blend II	117.06	0.9910
Blend III	117.66	1.0000
Blend IV	124.99	0.9885

quite close to that of sample A and, therefore, can be recommended for use in place of sample A.

3.7 Mass gain analysis

Certain physical and chemical activity such as adsorption of O₂ gas in porous structure of coal (mass gain), release of highly volatile hydrocarbon compounds from coal surface occurs (mass loss) during pre-ignition stage of combustion process. Corresponding effect is the variation of mass in TGA curve observed during pre-ignition stages as shown in Figs. 1 and 3. Reactivity of coal towards combustion process is a measure of net increase in mass with time duration of mass gain and temperature rise during pre-ignition stages. Lower mass gain across shorter time followed by ignition represents high reactivity of coal (Lee et al. 2012). Large weight gain across longer time and higher ignition temperature represents lower reactivity. Mass variation of sample A sample B and their blends were estimated from TGA/DTG data as shown in Fig. 1 and Fig. 3. Table 7 shows the variation in weight percentage during pre-ignition stages of combustion for sample A, sample B and their blends. Sample A has the lower gain (1.10 mass %) and lower time duration of 5.73 min, ($\Delta t = t_{\text{peak}} - t_{\text{start}}$ across a temperature range of 80 °C ($\Delta T = T_{\text{peak}} - T_{\text{start}}$) compared to sample B (1.18 wt%, 10.19 min, 120 °C during pre-ignition stages of combustion. That signifies sample A to be more reactive than sample B. However, for blends it

is observed that, weight gain is much higher (3.03%–3.62%) compared to sample A and B along with longer temperature range (120 °C). That implies pre-ignition reactivity of blends is lower compared to samples A and B.

4 Conclusions

The present work aims at analysing the combustion behaviour of a thermal coal (A) and a heat affected Jhama coal (B) and their blends using non-isothermal TGA. Sample A and Sample B were characterized by proximate analysis, ultimate analysis, GCV and free swelling index. Detailed analysis of various combustion temperature and characteristic parameters like ignition temperature, peak temperature and burnout temperature, ignition index, burnout index, combustion performance index rate and intensity index of combustion, activation energy were carried out. Experimental results show that sample A with 19% volatile matter content having lower burnout temperature of 484 °C compared to sample B with burnout temperature of 565 °C. Analysis of ignition index shows that sample A with D_i value of 5.30×10^{-3} wt% per min³ is easily combustible compared to sample B with D_i value of 2.76×10^{-3} wt% per min³. Combustion of coal blends with different mass ratios of sample A and sample B with 90:10, 80:20, 70:30 and 60:40 indicates that blending of thermal coal with heat affected Jhama coal at the ratio of 90:10 can be used in place of the thermal coal to reduce the fuel cost in the utilities.

Author contributions Experimental work carried out by Subhajit Aich under the guidance of Barun Kumar Nandi and Sumantra Bhattacharya.

Funding Work carried out by institute PhD students.

Data availability All the data has already been included in the manuscript.

Declarations

Table 7 Mass gains and characteristic temperature of coal

Sample	Weight (%)	<i>t</i> _{start} (min)	<i>t</i> _{peak} (min)	Δt (min)	<i>T</i> _{start} (min)	<i>T</i> _{peak} (min)	ΔT (min)
Sample A	1.10	19.64	27.73	5.73	250	330	80
Sample B	1.18	18.28	30.28	10.19	230	350	120
Blend I	3.03	15.49	27.48	10.03	210	330	120
Blend II	3.50	16.67	27.66	9.22	220	330	110
Blend III	3.96	17.10	30.1	11.67	220	350	130
Blend IV	3.62	18.57	27.05	6.59	240	325	85

Conflict of interest There is no such interest applicable in this manuscript.

Open Access This article is licensed under a Creative Commons Attribution 4.0 International License, which permits use, sharing, adaptation, distribution and reproduction in any medium or format, as long as you give appropriate credit to the original author(s) and the source, provide a link to the Creative Commons licence, and indicate if changes were made. The images or other third party material in this article are included in the article's Creative Commons licence, unless indicated otherwise in a credit line to the material. If material is not included in the article's Creative Commons licence and your intended use is not permitted by statutory regulation or exceeds the permitted use, you will need to obtain permission directly from the copyright holder. To view a copy of this licence, visit <http://creativecommons.org/licenses/by/4.0/>.

References

- Aich S, Behera D, Nandi BK, Bhattacharya S (2020) Relationship between proximate analysis parameters and combustion behaviour of high ash Indian coal. *Int J Coal Sci Technol*. <https://doi.org/10.1007/s40789-020-00312-5>
- Aich S, Nandi BK, Bhattacharya S (2019a) Utilization of sal leaves and sal leaves char to improve the combustion performance of reject coal. *Energy Sources Part A Recovery Util Environ Eff* 41:2299–2312
- Aich S, Nandi BK, Bhattacharya S (2019b) Effect of weathering on physico-chemical properties and combustion behavior of an Indian thermal coal. *Int J Coal Sci Technol* 6:51–62
- Alvarado PN, Cadavid FJ, Santamaría A, Ruiz W (2016) Reactivity and structural changes of coal during its combustion in a low-oxygen environment. *Energy Fuels* 30:9891–9899
- Baek SH, Park HY, HoKo S (2014) The effect of the coal blending method in a coal fired boiler on carbon in ash and NO_x emission. *Fuel* 128:62–70
- Behera D, Nandi BK, Bhattacharya S (2019) Chemical properties and combustion behavior of constituent relative density fraction of a thermal coal. *Energy Sources Part A Recovery Util Environ Eff* 41:654–664
- Behera D, Nandi BK, Bhattacharya S (2020) Studies on combustion characteristics of density by density analyzed coal. *J Energy Res Technol* 142:012301
- Chakladar S, Chakravarty S, Mohanty A, Alex TC, Kumar S (2020) Quality improvement of heat altered coals a preliminary feasibility study. *Environ Technol Innov* 18:100764
- Deng J, Ma X, Zhang Y, Li Y, Zhu W (2015) Effects of pyrite on the spontaneous combustion of coal. *Int J Coal Sci Technol* 2(4):306–311
- Ken BS, Aich S, Saxena VK, Nandi BK (2018) Combustion behaviour of KOH desulphurised coals assessed by TGA-DTG. *Energy Sources Part A Recovery Util Environ Eff* 40:2458–2466
- Lee DW, Bae JS, Park SJ, Lee YJ, Hong JC, Young-Chan Choi YC (2012) The pore structure variation of coal char during pyrolysis and its relationship with char combustion reactivity. *Ind Eng Chem Res* 51:13580–13588
- Li J, Zhu M, Zhang ZK, Shen G, Zhang D (2017) Effect of coal blending and ash temperature on ash sintering and fusion characteristics during combustion of Zhundong lignite. *Fuel* 195:131–142
- Lv C, Xu J, Xie H, Zeng Z, Wu Y (2006) Equilibrium strategy based coal blending method for combined carbon and PM10 emissions reductions. *Appl Energy* 183:1035–1052
- Nag D, Banerjee PK, Haldar SK (2011) Heat altered coal and its use in metallurgical coke making. *IJIS Int* 51(7):1194–1196
- Nag D, Singh AK, Banerjee PK (2009) Metallurgical use of heat altered coal a case study. *J Min Mater Charact Eng* 8:541–549
- Onifade M, Genc B (2019) Spontaneous combustion liability of coal and coal-shale: a review of prediction methods. *Int J Coal Sci Technol* 6(2):151–168
- Raaj SS, Arumugam S, Muthukrishnan M, Krishnamoorthy S, Anantharaman N (2016) Characterization of coal blends for effective utilization in thermal power plants. *Appl Therm Eng* 102:9–16
- Shih J, Frey HC (1995) Theory and methodology coal blending optimization under uncertainty. *Eur J Oper Res* 83:452–465
- Singh AK, Singh MP, Sharma M, Srivastava SK (2007) Microstructures and microtextures of natural cokes: A case study of heat-affected coking coals from the Jharia coalfield, India. *Int J Coal Geol* 71:153–175
- Singh AK, Sharma M, Singh MP (2016) Genesis of natural cokes: some Indian examples. *Int J Coal Geol* 75:40–49
- Wang D, Liang Q, Gong X, Liu H, Liu X (2017) Influence of coal blending on ash fusion property and viscosity. *Fuel* 189:15–22
- Zhang Y, Guo Y, Cheng F, Yan K, Cao Y (2015) Investigation of combustion characteristics and kinetics of coal gangue with different feedstock properties by thermogravimetric analysis. *Thermochim Acta* 614:137–148